

ARCH2S: Dataset, Benchmark and Challenges for Learning Exterior Architectural Structures from Point Clouds

Ka Lung Cheung^{1,2} Chi Chung Lee²

¹The Chinese University of Hong Kong ²Hong Kong Metropolitan University

klcheung@mae.cuhk.edu.hk, cclee@hkmu.edu.hk

<https://github.com/Semanticity-Research/ARCH2S>

Abstract

Precise segmentation of architectural structures provides detailed information about various building components, enhancing our understanding and interaction with our built environment. Nevertheless, existing outdoor 3D point cloud datasets have limited and detailed annotations on architectural exteriors due to privacy concerns and the expensive costs of data acquisition and annotation. To overcome this shortfall, this paper introduces a semantically-enriched, photo-realistic 3D architectural models dataset and benchmark for semantic segmentation. It features 4 different building purposes of real-world buildings as well as an open architectural landscape in Hong Kong. Each point cloud is annotated into one of 14 semantic classes.

1. Introduction

Detailed segmentation of exterior architectural structures, such as façades, elevations, and ground-level built objects, is crucial in various fields. It aids urban planning [14, 32], improves efficiency in construction [11, 15, 34, 40, 43], informs restoration efforts in heritage preservation [30, 31, 33], and advances technologies such as autonomous vehicles [5, 7, 48] and drone navigation systems [4, 8, 25, 26] by providing a semantic view of the surroundings [35].

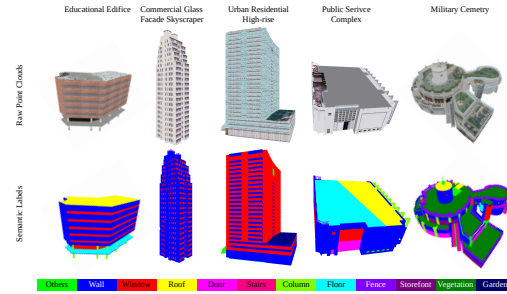


Figure 1. Point cloud models from ARCH2S dataset. Different colors label different semantic classes.

Despite advancements in LiDAR scanning technology and the rise of large-scale 3D point cloud datasets, capturing a comprehensive view of exterior architectural structures remains a challenge [21, 41]. Specifically, the outdoor roadway-level datasets [18, 20, 22, 28, 48, 49] often abstract the (large-sized) buildings as single entities, finer details of exteriors due to sensory gap [13]. Although a recent surge of façade-level datasets [24, 42, 46] have aimed to address this problem by identifying the architectural parts on the building’s vertical and planar wall surfaces, ground-level and rooftop-level exterior structures are disregarded. Considering the above data hunger problem [13] and increasing adoption of Building Information Modeling (BIM) [12, 23, 34, 37], a 3D architectural models dataset with rich annotations on every (level, angle) of the exterior surface is pressingly needed,

which provides detailed categorization and distinction of different structural features.

In this paper, we present a richly annotated, semantically-enriched 3D **Architectural** models dataset – ARCH2S. Our dataset (*cf.* Fig. 1) includes Semantic Segmentation benchmark for learning exterior architectural structures. It contains real-world reconstruction scenes with photorealistic texture through texture mapping techniques. The dataset includes prominent buildings in Hong Kong and a historical open landscape. The significance of our dataset is summarized as follows:

- Unlike the extensively researched outdoor roadway and façade-level datasets, our dataset covers detailed annotations of real-world reconstructed exterior building objects into 13 commonly seen built elements grouped into three main categories (miscellaneous, structural, and decorative) (*cf.* Fig. 5). The broad spectrum of semantic classes creates fine-grained annotation on the façades, roof, and ground-level objects.
- Being reconstructed from oblique aerial images, our point cloud models feature a polyhedral footprint and rooftop structures enhanced with photorealistic textures. Meanwhile, our dataset is evaluated with the state-of-the-art algorithms in the 3D segmentation task. Through evaluation of the annotation (*cf.* Fig. 4) and benchmark results (*cf.* Tab. 1), we discuss the challenges (*cf.* Sec. 3) in annotation and semantic segmentation for large-sized 3D architectures.

2. The ARCH2S Dataset

Our dataset contains prominent buildings and an open landscape from Hong Kong for five different architectural purposes: educational, residential, commercial, public service, and military cemetery (*i.e.* the open landscape) architecture. We randomly sampled approximately 5M points for each scene from a mesh object source to generate point cloud models. These models are annotated with 13 commonly seen structural and decorative built object classes, along with an extra class (“Others”) for architectural components that do not fit into the pre-determined 13 classes (*cf.* Fig. 5).

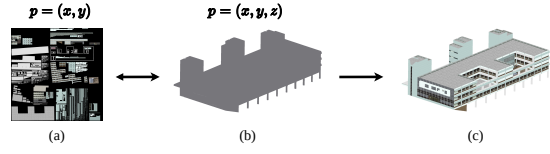


Figure 2. Illustration of the stages of UV mapping with our mesh (Educational Facility). (a) The UV layout with 2D coordinates (x, y) , representing each point p on the mesh’s surface. (b) The 3D mesh in gray-scale, showing points p in 3D space (x, y, z) for texture projection. (c) The final textured mesh, with the UV map applied, displays detailed and colored surfaces.

2.1. Dataset Preparation

Models Mining. Our 3D models are derived from the 3DBIT00 dataset [2] provided by the Hong Kong Lands Department [1]. The dataset is updated bi-monthly and features individualized 3D models with geometric shapes, appearance, and position of three types of ground objects: buildings, infrastructure, and terrain. Our project extracted targeted FBX formatted models (mesh models), which were to be annotated by human operators. Additionally, we selected an extra Educational Facility model (*cf.* Figs. 2 to 4). This served as a sample for annotator training and to benchmark annotators’ performance.

Mesh Pre-processing. The FBX building meshes were provided with a UV texture map. This map assigns a 2D image to a set of coordinates, where U represents the horizontal axis, and V represents the vertical axis. By employing UV mapping (*i.e.* texture mapping [9, 39]), as shown in Fig. 2 (a-c), the object appearances (*e.g.* color, texture, and pattern) were incorporated into the surface of our 3D meshes.

Point Sampling from Mesh. After completing the UV mapping, we generated a point cloud on the UV-mapped 3D mesh, shown in Fig. 3. This was achieved by randomly sampling (5M) points on the surface of the mesh model. We set a target of 5M sampling points to maintain data granularity

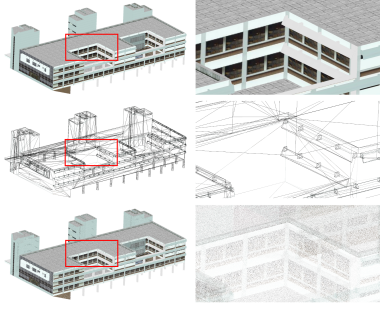


Figure 3. Illustration of the random point sampling on our mesh. Plain mesh (top), wireframe display (middle), and corresponding sampled points (bottom).

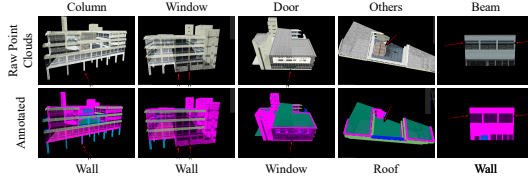


Figure 4. Comparative analysis of raw point cloud data and semantic annotations in the Educational Facility, visualized on the annotation interface. The top row displays raw point cloud representations, while the bottom row shows the semantically annotated elements with various colors denoting different labeled classes. Red arrows indicate discrepancies where the semantic labels do not accurately match the actual built elements, highlighting areas of potential mislabeling.

while minimizing data volume to ensure a successful loading into the annotation interface. The color information from the original mesh was collected by interpolating this data within each triangle. Each randomly positioned point adopted the properties of the UV coordinates at its location, thus preserving the visual details from the texture map.

2.2. Benchmarks

Train and Test Splits. We define standard training and testing splits so that no duplicates occur between train and test splits. We first trained with Educational, Residential, and Public Service buildings and Military cemetery and tested on Commercial buildings. Each building model is downsam-

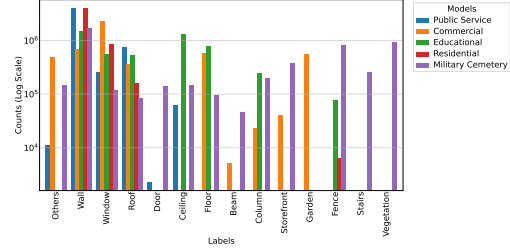


Figure 5. The distribution of different semantic categories in ARCH2S dataset. Our dataset, consisting of 14 out of 22 semantic classes, covers a diverse range of common exterior architectural elements. Note that the “Garden” semantic label is reported only in the Commercial Centre point cloud. Moreover, point counts are on a logarithmic scale for the vertical axis.

pled into grid boxes of 0.75×0.75 m and hashed with voxel hashing [47], which includes the global geometries and RGB values for point clouds.

Representative Baselines. Neural segmentation methods in scene semantic segmentation include, but are not limited to, two mechanisms: convolution-based [10, 36] and the recent point-wise transformer-based [44, 45, 50] methods. We have selected five representative methods as solid baselines for benchmarking our dataset. The candidate models from convolution-based methods include SpUNet [10, 36] and MinkUNet [10], while transformer-based methods include PTv1 [50], PTv2 [45], and PTv3 [44].

Evaluation Metrics. Similar to existing benchmarks [6, 17], we use Overall Accuracy (OA) and mean Intersection-over-Union (mIoU) as the primary evaluation metrics.

3. Results and Discussion

Challenges in Annotation. Despite providing the training and instructions to the annotators, We report a few potential mislabeled objects in the annotated model generated by the human operators (*cf.* Fig. 4) compared to the raw point cloud scene in the training phase. The inconsistencies in labeling are intelligible, considering the semantic

Table 1. Quantitative results of five selected baselines on ARCH2S dataset Overall Accuracy (OA, %), mean class Accuracy (mAcc, %), mean IoU (mIoU, %), and per-class IoU (%) are reported. Miscellaneous: built element that belongs inclusively into decorative and structural categories. All baselines are trained from scratch (without pre-trained weights). The best and second-best results within each metric are denoted in **red** and **blue**, respectively.

Methods	OA (%)	mAcc (%)	mIoU (%)	Miscellaneous							Structural				Decorative		
				Others	Wall	Window	Door	Roof	Storefront	Ceiling	Floor	Beam	Stairs	Column	Fence	Vegetation	Garden
SpUNet	30.98	14.8	6.45	0.79	21.75	24.66	0.00	24.77	32.18	0.00	0.00	0.00	0.00	18.03	0.00	0.00	0.00
MinkUNet	32.31	15.28	7.39	0.00	20.43	7.5	0.00	38.98	13.45	0.00	60.01	0.00	0.00	0.00	0.00	0.00	0.00
PTv1	48.64	5.94	3.44	7.42	6.06	51.91	0.00	0.00	0.00	0.00	0.00	0.00	0.00	0.00	0.00	0.00	0.00
PTv2	18.50	7.95	3.16	0.00	18.72	0.94	0.00	0.00	16.84	0.00	23.57	0.00	0.00	0.00	0.00	0.00	0.00
PTv3	22.59	10.07	3.01	0.09	19.91	8.05	0.00	24.30	4.85	0.00	0.00	0.00	0.00	0.00	0.00	0.00	0.00

gaps from annotators [13]. Annotators have different viewpoints or ambiguous definitions when classifying the building components (*e.g.* classes: {“Column”, “Beam”, “Wall”}, classes: {“Floor”, “Fence”, “Window”}, classes: {“Roof”, “Ceiling”}).

Learning Exterior Architectural Structures.

Tab. 1 shows the convolutional methods outperform Vision Transformers (ViTs) in terms of mIoU across various categories. SpUNet [10, 36] and MinkUNet [10] are able to learn richer local features on neighborhood points and handle the sparsity of large-scale point clouds efficiently [16, 19], resulting with greater generalization compared to PTv1 [50], PTv2 [45], and PTv3 [44]. Conversely, ViTs result poorly primarily due to the lack of locality, inductive biases, and hierarchical structure of the representations [16, 27, 29, 38] when processing with large data grids. Thus, high-capacity models like ViTs are seen to be less efficient when trained with our dataset.

Impact of Imbalanced Semantic Distribution.

The segmentation performance in building classes varies, with dominant classes performing better than underrepresented, minor classes. Major structures like “Wall” and “Window” result in a higher per-class IoU score (*cf.* Tab. 1) than the minority, suggested by their scene occupation and class dominance. These class objects appear to have large

planar surfaces (*i.e.* large amount of points on the same class), which bring scant novel information to scene understanding. In contrast, segmenting those minority classes (*e.g.* “Beam” and “Column”) is challenging due to under-representation, leading to less accurate segmentation (*i.e.* significantly low or nearly zero per-class IoU). Additionally, minor class objects inherently have more complex, varied shapes, styles, and patterns than other major class objects, which poses additional challenges to model generalization. To improve the semantic learning of the building model, transfer learning [3] or different class-weighted loss functions [3, 20] are possible solutions to mitigate the impact of long-tail data distribution [13].

4. Conclusion

In this paper, we introduced a semantically-enriched 3D architectural models dataset with varied semantic classes for the commonly seen building components. Through our analyses of annotations and benchmarking results, We identified several open challenges: 1) inconsistent annotations for complex architecture due to the semantic gap, 2) the issue of model generalization, and 3) the impact of the imbalanced class distribution. Despite these challenges, our dataset aspires to be pioneering work to encourage the adoption of BIM and novel applications related to smart cities.

References

- [1] Lands department - the government of the hong kong special administrative region. 2
- [2] 3d spatial data 3d-BIT00 | DATA.GOV.HK. 2
- [3] Saleh Abu Dabous and Sainab Feroz. Condition monitoring of bridges with non-contact testing technologies. 116:103224. 4
- [4] Ahmad Alsayed, Akilu Yunusa-Kaltungo, Mark K. Quinn, Farshad Arvin, and Mostafa R. A. Nabawy. Drone-assisted confined space inspection and stockpile volume estimation. 13(17):3356. 1
- [5] Jaehoon Bae, Jonghoon Lee, Arum Jang, Young K. Ju, and Min Jae Park. SMART SKY EYE system for preliminary structural safety assessment of buildings using unmanned aerial vehicles. 22(7): 2762. 1
- [6] Jens Behley, Martin Garbade, Andres Milioto, Jan Quenzel, Sven Behnke, Cyrill Stachniss, and Juer-gen Gall. SemanticKITTI: A dataset for semantic scene understanding of LiDAR sequences. 3
- [7] Anushka Biswas and Hwang-Cheng Wang. Autonomous vehicles enabled by the integration of IoT, edge intelligence, 5g, and blockchain. 23(4): 1963. 1
- [8] Michele Bolognini, Giovanni Izzo, Daniele Marchisotti, Lorenzo Fagiano, Maria Pina Limon-gelli, and Emanuele Zappa. Vision-based modal analysis of built environment structures with multiple drones. 143:104550. 1
- [9] Catmull, E. A subdivision algorithm for computer display of curved surfaces | computer science archive. 2
- [10] Christopher Choy, JunYoung Gwak, and Silvio Savarese. 4d spatio-temporal ConvNets: Minkowski convolutional neural networks. 3, 4
- [11] Valeria Croce, Gabriella Caroti, Livio De Luca, K vin Jacquot, Andrea Piemonte, and Philippe V ron. From the semantic point cloud to heritage-building information modeling: A semiautomatic approach exploiting machine learning. 13(3):461. 1
- [12] Amos Darko, Albert P.C. Chan, Yang Yang, and Mershack O. Tetteh. Building information modeling (BIM)-based modular integrated construction risk management – critical survey and future needs. 123:103327. 1
- [13] Biao Gao, Yancheng Pan, Chengkun Li, Sibogeng, and Huijing Zhao. Are we hungry for 3d LiDAR data for semantic segmentation? a survey and experimental study. 1, 4
- [14] Weixiao Gao, Liangliang Nan, Bas Boom, and Hugo Ledoux. PSSNet: Planarity-sensible semantic segmentation of large-scale urban meshes. 196: 32–44, . 1
- [15] Ning Gu and Kerry London. Understanding and facilitating BIM adoption in the AEC industry. pages 988–999. 1
- [16] Yulan Guo, Hanyun Wang, Qingyong Hu, Hao Liu, Li Liu, and Mohammed Bennamoun. Deep learning for 3d point clouds: A survey. 4
- [17] Timo Hackel, Nikolay Savinov, Lubor Ladicky, Jan D. Wegner, Konrad Schindler, and Marc Polle-feys. Semantic3d.net: A new large-scale point cloud classification benchmark. 3
- [18] Niklas Hanselmann, Katrin Renz, Kashyap Chitta, Apratim Bhattacharyya, and Andreas Geiger. KING: Generating safety-critical driving scenarios for robust imitation via kinematics gradients. 1
- [19] Yong He, Hongshan Yu, Xiaoyan Liu, Zhengeng Yang, Wei Sun, and Ajmal Mian. Deep learning based 3d segmentation: A survey. 4
- [20] Qingyong Hu, Bo Yang, Sheikh Khalid, Wen Xiao, Niki Trigoni, and Andrew Markham. Towards semantic segmentation of urban-scale 3d point clouds: A dataset, benchmarks and challenges. 1, 4
- [21] Jin Huang, Jantien Stoter, Ravi Peters, and Liangliang Nan. City3d: Large-scale building reconstruction from airborne LiDAR point clouds. 14 (9):2254. 1
- [22] Peng Jiang, Philip Osteen, Maggie Wigness, and Srikanth Saripalli. RELIS-3d dataset: Data, benchmarks and analysis. version: 4. 1
- [23] Ehsan Kamel and Ali M. Memari. Review of BIM’s application in energy simulation: Tools, issues, and solutions. 97:164–180. 1
- [24] Pierre-Alain Langlois, Yang Xiao, Alexandre Boulch, and Renaud Marlet. VASAD: a volume and semantic dataset for building reconstruction from point clouds. In *2022 26th International Conference on Pattern Recognition (ICPR)*, pages 4008–4015. IEEE. 1
- [25] Fangyu Li, Sisi Zlatanova, Martijn Koopman, Xueying Bai, and Abdoulaye Diakite. Universal path planning for an indoor drone. 95:275–283. 1
- [26] Han Liang, Seong-Cheol Lee, Woosung Bae, Jeongyun Kim, and Suyoung Seo. Towards UAVs in construction: Advancements, challenges, and future directions for monitoring and inspection. 7(3): 202. 1

- [27] Yahui Liu, Enver Sangineto, Wei Bi, Nicu Sebe, Bruno Lepri, and Marco Nadai. Efficient training of visual transformers with small datasets. In *Advances in Neural Information Processing Systems*, pages 23818–23830. Curran Associates, Inc. 4
- [28] Romain Loiseau, Mathieu Aubry, and Loïc Landrieu. Online segmentation of LiDAR sequences: Dataset and algorithm. 1
- [29] Dening Lu, Qian Xie, Mingqiang Wei, Kyle Gao, Linlin Xu, and Jonathan Li. Transformers in 3d point clouds: A survey. 4
- [30] Francesca Matrone and Massimo Martini. Transfer learning and performance enhancement techniques for deep semantic segmentation of built heritage point clouds. 12(25):73. 1
- [31] F. Matrone, A. Lingua, R. Pierdicca, E. S. Malinverni, M. Paolanti, E. Grilli, F. Remondino, A. Murtiyoso, and T. Landes. A BENCHMARK FOR LARGE-SCALE HERITAGE POINT CLOUD SEMANTIC SEGMENTATION. XLIII-B2-2020: 1419–1426. 1
- [32] Aisyah Marliza Muhmad Kamarulzaman, Wan Shafrina Wan Mohd Jaafar, Mohd Nizam Mohd Said, Siti Nor Maizah Saad, and Midhun Mohan. UAV implementations in urban planning and related sectors of rapidly developing nations: A review and future perspectives for malaysia. 15 (11):2845. 1
- [33] E. Pellis, A. Murtiyoso, A. Masiero, G. Tucci, M. Betti, and P. Grussenmeyer. AN IMAGE-BASED DEEP LEARNING WORKFLOW FOR 3d HERITAGE POINT CLOUD SEMANTIC SEGMENTATION. XLVI-2/W1-2022:429–434. 1
- [34] Phillip Schönfelder, Angelina Aziz, Benedikt Faltin, and Markus König. Automating the retrospective generation of as-is BIM models using machine learning. 152:104937. 1
- [35] Pratheba Selvaraju, Mohamed Nabail, Marios Loizou, Maria Maslioukova, Melinos Averkiou, Andreas Andreou, Siddhartha Chaudhuri, and Evangelos Kalogerakis. BuildingNet: Learning to label 3d buildings. In *2021 IEEE/CVF International Conference on Computer Vision (ICCV)*, pages 10377–10387. IEEE. 1
- [36] Spconv Contributors. Spconv: Spatially sparse convolution library. original-date: 2019-01-19T02:57:09Z. 3, 4
- [37] Shu Tang, Dennis R. Shelden, Charles M. Eastman, Pardis Pishdad-Bozorgi, and Xinghua Gao. A review of building information modeling (BIM) and the internet of things (IoT) devices integration: Present status and future trends. 101:127–139. 1
- [38] Yi Tay, Mostafa Dehghani, Dara Bahri, and Donald Metzler. Efficient transformers: A survey. 4
- [39] Tecgraf Institute of PUC-Rio. 5 texture mapping. 2
- [40] Rebekka Volk, Julian Stengel, and Frank Schultmann. Building information modeling (BIM) for existing buildings — literature review and future needs. 38:109–127. 1
- [41] Ruisheng Wang, Shangfeng Huang, and Hongxin Yang. Building3d: An urban-scale dataset and benchmarks for learning roof structures from point clouds. In *2023 IEEE/CVF International Conference on Computer Vision (ICCV)*, pages 20019–20029. IEEE. 1
- [42] WHU. WHU-TLS_benchmark_dataset-1. 1
- [43] Wiley. BIM handbook: A guide to building information modeling for owners, designers, engineers, contractors, and facility managers, 3rd edition | wiley. 1
- [44] Xiaoyang Wu, Li Jiang, Peng-Shuai Wang, Zhijian Liu, Xihui Liu, Yu Qiao, Wanli Ouyang, Tong He, and Hengshuang Zhao. Point transformer v3: Simpler, faster, stronger, . version: 1. 3, 4
- [45] Xiaoyang Wu, Yixing Lao, Li Jiang, Xihui Liu, and Hengshuang Zhao. Point transformer v2: Grouped vector attention and partition-based pooling, . version: 2. 3, 4
- [46] Olaf Wysocki, Ludwig Hoegner, and Uwe Stilla. TUM-FA\c{C}ADE: Reviewing and enriching point cloud benchmarks for fa\c{c}ade segmentation. XLVI-2/W1-2022:529–536. 1
- [47] Yi Xu, Yuzhang Wu, and Hui Zhou. Multi-scale voxel hashing and efficient 3d representation for mobile augmented reality. In *2018 IEEE/CVF Conference on Computer Vision and Pattern Recognition Workshops (CVPRW)*, pages 1586–15867. IEEE. 3
- [48] Shanliang Yao, Runwei Guan, Xiaoyu Huang, Zhuoxiao Li, Xiangyu Sha, Yong Yue, Eng Gee Lim, Hyungjoon Seo, Ka Lok Man, Xiaohui Zhu, and Yutao Yue. Radar-camera fusion for object detection and semantic segmentation in autonomous driving: A comprehensive review. pages 1–40. 1
- [49] Xiangyu Yue, Bichen Wu, Sanjit A. Seshia, Kurt Keutzer, and Alberto L. Sangiovanni-Vincentelli. A LiDAR point cloud generator: from a virtual world to autonomous driving. In *Proceedings of the 2018 ACM on International Conference on Multimedia Retrieval*, pages 458–464. ACM. 1

- [50] Hengshuang Zhao, Li Jiang, Jiaya Jia, Philip Torr, and Vladlen Koltun. Point transformer. [3](#), [4](#)